Journal of Kufa for Chemical Sciences
ISSN(P) :2077-2351 ISSN(E): 3006-3280
Journal Homepage:
https://journal.uokufa.edu.iq/index.php/jkcs/index

Article

Synthesis, Characterization of some Metallic Complexes and Exploring the Anticancer Activity of Au(III) Complex with Newly Ligand drived from xanthine compounds

Majida Ibrahim Obaid*1 , Ibtihal Kadhim Kareem2, Wurood Ali Jaafar3

1,2 Chemistry department/ faculty of Education for women/ University of Kufa .

3Chemistry department/ faculty of Education for Pure Sciences – Ibn AL Haitham/ University of Baghdad.

*1Majidai.alshammary@student.uokufa.edu.iq

2 ibtihal.dosh@uokufa.edu.iq

3 wurood.a.j@ihcoedu.uobaghdad.edu.iq

Abstract:

The new Azo-Schiff ligand8-((1E)-(2-(((4-hydroxy-3-methoxybenzylidene)amino)methyl)phenyl)diazenyl)-1,3,7-trimethyl-3,7-dihydro-1H-purine-2,6-dione was prepared from Ortho-aminobenzylamine azoate and reaction with Caffeine, followed by the condensation of the resulting compound withVanillin . Different analytical and characterization techniques including (FT-IR, UV-Vis. Spectroscopy, GC-mass, ^{1}HNMR and C.H.N elemental analysis) in the investigation of newly prepared ligand. A series of novel solid metal complexes of this ligand with Cu (II),Ag(I) and Au(□) were prepared and all complexes were characterization by techniques above, excluding the mass and the ^{1}H-NMR spectroscopy of some prepared solid metal complexes and the use of flame atomic absorption spectroscopy to determine the percentages of metal ions in the prepared complexes and molar conductivity of the metal complexes dissolved in DMSO at 1 × 10^{-3} M concentration laboratory temperature. The results of this studies showed that the coordination sites for the new Azo-Schiff base ligand with Cu (II), Ag (I) were to be through nitrogen of the Caffeine ring, ,the nitrogen of azo group and the

nitrogen of azomethine group . The Electronic spectral and magnetic measurement data predict octahedral structure of the Cu (II),tetrahedral of the Ag (I) complexe while it has a square planar shape with the Au(III) ion. All complexes have electrolytic properties . Significant antiproliferative activity was seen in it against human lung cancer (A549) and normal cell lines (HDFn), as evidenced by the IC50 values. This study could contribute to the development of pharmaceutical preparations.

Keywords: Gold complex, lung cancer, Xanthines

Introduction

Azo-imine derivatives are chemical combinations that have attracted much interest in scientific research compared to imine chemicals and azo dyes [1]. Azo-imines are essential because to their structural, electronic, flexibility, and selectivity qualities to metal ions [2 - 3]. This is due to the presence of two reactive groups, -N=CH- and -N=N- [4]. These molecules are ligands, which can be coordinated in a variety of ways. They can coordinate via nitrogen atoms of azo and imine groups [5], or by nitrogen of azo group alone, and ultimately via nitrogen atoms of azo imine [6].

Xanthines are purine bases, which are known to act as non-selective and multitargeting agents of several cellular proteins [7]. Some xanthines play a role as bronchodilators [8]. Furthermore, xanthines were studied for their activity as cancer chemotherapy adjuvants[9] . Numbers of xanthine analogs have been synthesized and introduced to obtain more selective and potent agents for use as research tools and as possible therapeutic agents[10]. The adopted substitutions (methyl or alkyl) at several positions and chemical spaces around the xanthine motif played a major involvement in the tumor microenvironment.

EXPERIMENTAL SECTION

Materials and Instrumentation

The materials, 2-amino benzylamine, silver nitrate and hydrochloric acid were purchased from Sigma Aldrich Chemical Company in England4-Floro benzaldehyde were from Fluka Company. Copper(II) chloride dihydrate,gold sodium chloride (□) from micklin, methanol, ethanol from B.D.H Company. Benzene was from G.C.C. Company. Absolute ethanol was from Sharlut Company. Dimethyl sulfoxide (DMSO) was from A.C.S. Company. Glacial acetic acid was from Merck Chemical Company. All these chemicals used were utilized as received without any further purification.Instrumentation Melting points were measured using Type Shanghai

Drawell Scientific Instrument for ligands and their complexes. ^{1}H-NMR spectra were acquired as solutions in DMSO-d6 solvent applying a Varian 500 MHz spectrophotometer while the mass spectra were recorded on a GCMS-QP2010SE:ShimadzuSpectrometer. The Shimadzu Visible-Uv Spectrophotometer (Shimadzu UV-160PC) was used for recording UV-vis spectra. Magnetic susceptibility measurements were performed using the Faraday method with a balanced magnet MSB-MKI. Diamagnetic correction using Pascal's constant. Infrared (IR) spectra were measured using a Shimadzu FTIR 8400 spectrometer utilizing KBr in the 4000–400 cm^{-1} wavelength range. C.H.N elemental analysis was studied using C.H.N elemental analyzer (EURO 2012EA 300). Used field emission scanning electron scanning device (FESEM) was used to take a very magnified image of the large magnification (120.00 kX) of the device for the eyes to use (TESCAN, Germany), XRD bruker from Germany was used for recording X-ray diffraction.

The devices manufacture's name/state and type of equipment used for toxicological studies are Centrifuge Cooling, Eppendorf (Germany) ; Inverted Microscope , Olympus (Japan); CO_2 incubator, Gallenkamp (England); Laminar Air Flow, K and K (Korea); Micro-titer Plate Reader, Bio-Rad (Germany); Sensitive Balance, Sartorius (Germany); Haemocytometer, Sigma (USA); ELISA reader, Thermofisher(Japan).

Synthesis of the new Azo- Schiff base ligand

The first step included preparing the azo dye (0.01 mol, 1.22g) of ortho-aminobenzylamine was dissolved in (30mL) of distilled water, while keeping the temperature of the reaction medium low between (0-5□). After that, (5mL) was added of concentrated HCl acid with continuous shaking of the solution. Likewise, (0.01 mol, 0.70g) of $NaNO_2$ was dissolved in (5mL) of distilled water and the solution was cooled to below zero degrees Celsius, after which the second cooled solution was added to the aromatic amine solution with shaking and stirring and the solution was left for (30 minutes) for the purpose Completion of the azotization process, This was followed by adding the diazonium salt solution drop by drop, with continuous stirring, to the compound solution, which consists of (0.01 mol, 1.94 g) Caffeine and (20mL) of sodium bicarbonate solution (40 % $NaHCO_3$) with the addition of (50mL) of ethanol, at a temperature (0□) with continuous stirring and at (pH ≈7) by monitoring with PH paper, the resulting solution was left for 24 hours to complete the precipitation process, then the formed azo was filtered, washed with distilled water several times, dried, and recrystallized using hot absolute ethanol[11]. The second step included preparing the new ligand azo - Schiff base, by

dissolving (0.002 mol, 0.42 g) of Vanillin in (10 mL) of absolute ethanol, and stirring for (2 minutes), then adding (2-3) drops of glacial acetic acid, then left for (5 minutes) at laboratory temperature. After that, a solution prepared from dissolving (0.002 mol, 0.92g) of azo dye in (20 mL) of absolute ethanol is added, and it is heated. The solution lasted for (16 hrs) at a temperature of (78□), and the new azo ligand - Schiff base was obtained. The product was dried, collected, and then recrystallized using hot absolute ethanol[12]. Its physical properties were listed in Table (1). Schem shows the steps for preparing the azo ligand - the new Schiff base.

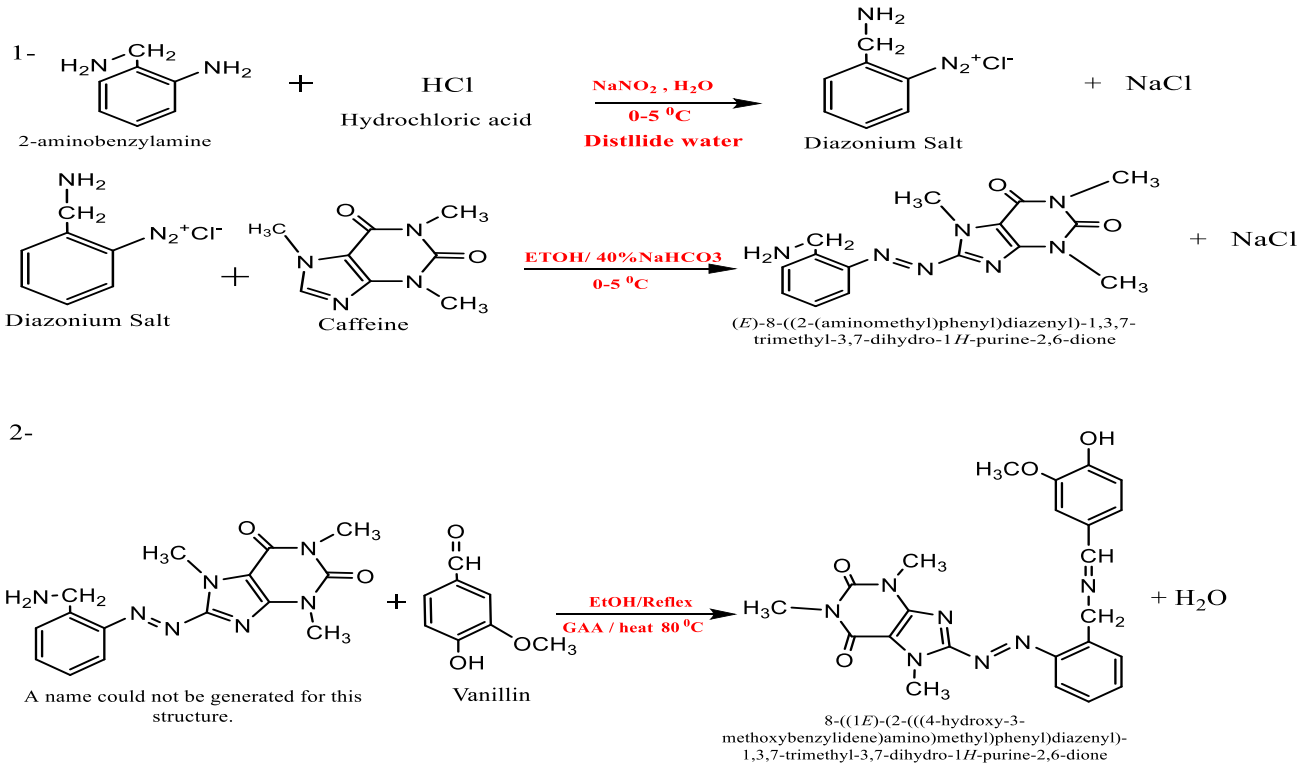

Schem:1. Synthesis of new azo-Schiff base ligand

Synthesis of metal complexes:

The metal complexes were synthesized by mixing of (0.0004 mol) in 10 ml absolute ethanol solution of each of $CuCl_2.2H_2O$ and $AgNO_3$ with 10 ml absolute ethanol solution of (0.2g, 0.0004mol) of new Azo-Schiff base ligand in (1:1) (metal: ligand) ratio. The resulting mixture was refluxed for 3h. The products obtained were cooled, dried, and recrystallized through hot absolute ethanol[13]. The physical properties of the complexes under study are listed in Table 1.Scheme :2 illustrates the steps of preparing the metal complexes with the ligand.

Preparation of nano-gold complex $[Au(L)Cl]Cl_2$

The preparing of $[Au(L)Cl]Cl_2$ complex includes adding 0.21 g (0.0006 mol) of $NaAuCl_4$ in 10 mL absolute ethanol solution of 1:1 (metal: ligand) molar ratio to 0.3

g (0.0006 mol) of L, after adding 10 mL. The resulting solution was refluxed for 25 h. The product obtained was cooled, dried, and recrystallized through hot absolute ethanol[14].

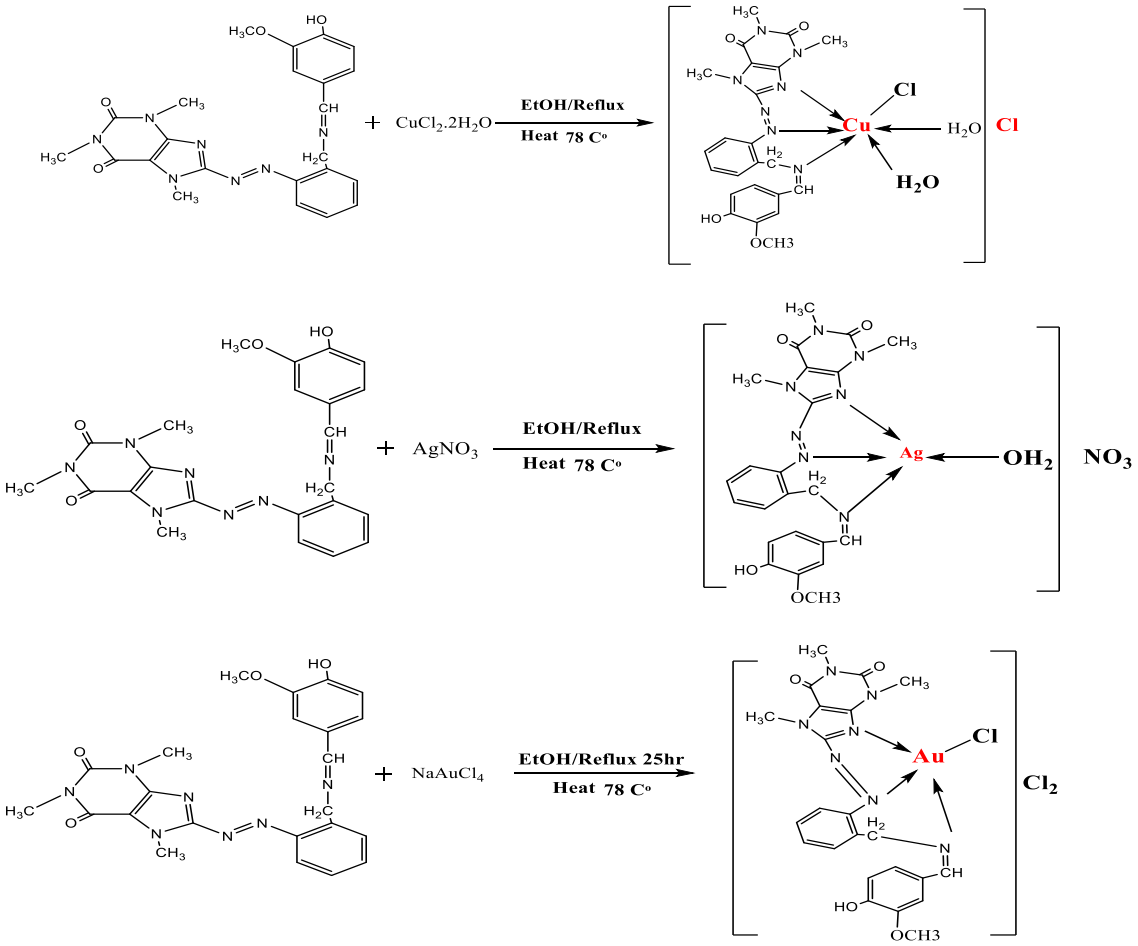

Scheme: 2 . Synthesis of the new ligand metal complexes Cu(□),Ag(□) ,Au(□)

Table: 1. Shows the physical properties of the new Azo Schiff base ligand and its complexes.

No.	Chemical formula	M.Wt g/mol	Color	M.PC°	Yield %
1.	$C_{23}H_{23}N_7O_4$	461.48	Brown	70-72	75%
2.	$[Cu(L)Cl(H_2O)_2]Cl$	632.02	Yellowish brown	123-125	91%
3.	$[Ag(L)H_2O]NO_3$	649.34	Dark brown	153-155	84%
4.	$[Au(L)Cl]Cl_2$	764.94	Reddish brown	250 >	71%

In vitro cell cytotoxicity and viability assays Development of lung cancer cell line (A549- cells).

Lung cancer cells have demonstrated a favorable response to gold complexes [15]. to get healthy and malignant cell lines ready for research. A white man with lung cancer, aged 58, had lung tissue from which the A549 cell line was extracted. Research on cancer, immuno-oncology, and toxicity can all make use of this cell line. Isolated from neonatal foreskin, Primary Dermal Fibroblast Normal; Human, Neonatal (HDFn) is a cell line with potential uses in studies on pathogen response, skin aging, wound healing, gene delivery, and skin conditions like scleroderma. These cell lines were acquired from the Medicine College's Pharmacology Department at Malaya University in Kualalampur, Malaysia. The MTT ready-to-use kit (Intron Biotech) was used to test the cytotoxic effects of $[Au(L)Cl]Cl_2$ compounds at varying concentrations.

Procedure:

In 96 flat-well micro-titer plates, tumor cells (1×10^4–1×10^6 cells/ml) were cultivated in a final volume of 200 µl of full culture media each well. After covering the microplate with sterile parafilm, it was carefully shacked. The plates were incubated for 24 hours at 37°C with 5% CO_2. Following incubation, the medium was taken out and the wells were filled with two-fold serial dilutions of the compounds (400, 200, 100, 50, and 25 µg/ml). Both the controls (cells treated with serum free media) and each concentration were utilized in triplicate. For a chosen exposure duration of four hours, plates were incubated at 37°C with 5% CO_2. For 24 hours, 20 µl of each component was added to each well. For the chosen exposure period of four hours, plates were incubated at 37°C with 5% CO_2. For 24 hours, 20 µl of each compound was added to each well. Each well received 10 µl of the MTT solution upon exposure. The plates were then incubated for four hours at 37°C with 5% CO_2. After carefully removing the media, 100 l of solubilization solution was poured to each well and left for five minutes. An ELISA reader operating at 575 nm was used to measure the absorbance. The following formula was used to statistically analyze the optical density data and determine the concentration of chemicals needed to reduce cell viability by 50% for each cell line: Y = 1+10 (x-logC)B / D+ A-D [16].

RESULTS AND DISCUSSION

Excellent solubility in different solvents was tested for metallic complexes such as DMF, DMSO, MeOH, and EtOH. Additionally. These metal complexes and the ligand were studied using various analytical methods, including fine analysis of

elements, molar electrical conductivity, infrared, UV-vis, mass spectrum measurement, and NMR (only ligand measured). The experimental results and analytical data of the complexes are in good agreement, confirming their accuracy. Based on the data shown in Table 3, specifically, the results of precise element analysis (C.H.N) and molar conductivity measurements were adopted molar ratio was 1:1(M:L) of the complexes Cu(II), Ag(I) and Au(III) , where the tridentate ligand coordinates with metal ions through 3 sites (N,N,N) to form an octahedral shape in Cu(II) and tetrahedral in Ag(I) complex, while in the gold complex the tridentate ligand coordinates with Au(III) ion through the coordination sites mentioned above to take square planar geometry. Thus, the surrounding ligands coordinate around the core metal ions. This aligns with what has been mentioned in previous literature regarding this type of complex [17]. The chelate complexes synthesized in this study exhibited significant conductivity levels, demonstrating that complexes exhibit an electrolytic character.

Mass Spectra

Mass spectrometry is one of the essential and crucial diagnostic tools through which the molecular weight and molecular formula of new compounds can be proven[18] . The mass spectrum of the new organic ligand and gold complex were measured using mass spectrometry. Show the mass spectrum of the organic ligand molecular ion (M/Z+) at (461) and the gold complex of the molecular ion (M/Z+) was observed at (765) [19].

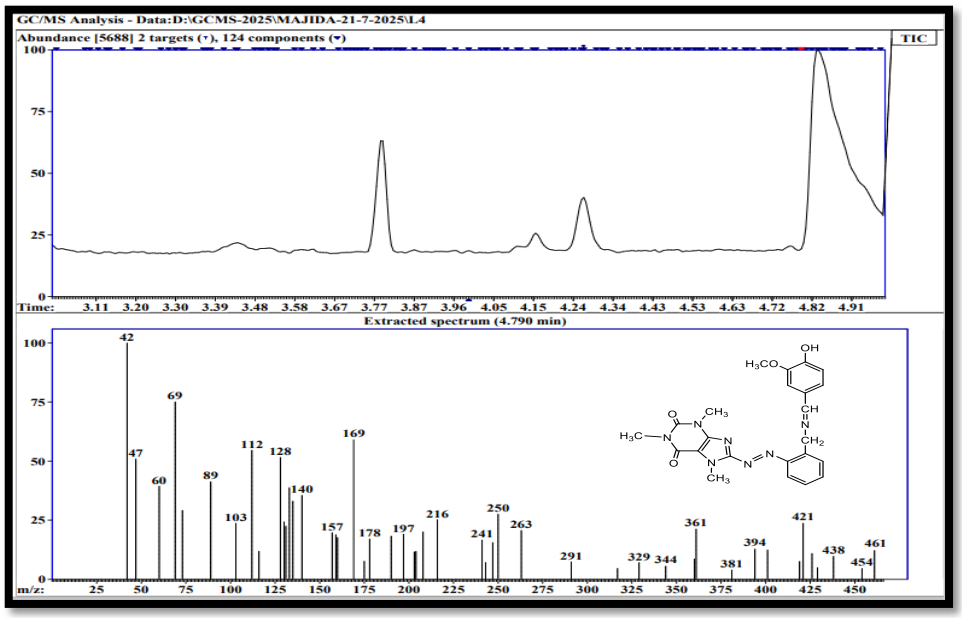

Fig 1. Mass spectrum of the ligand

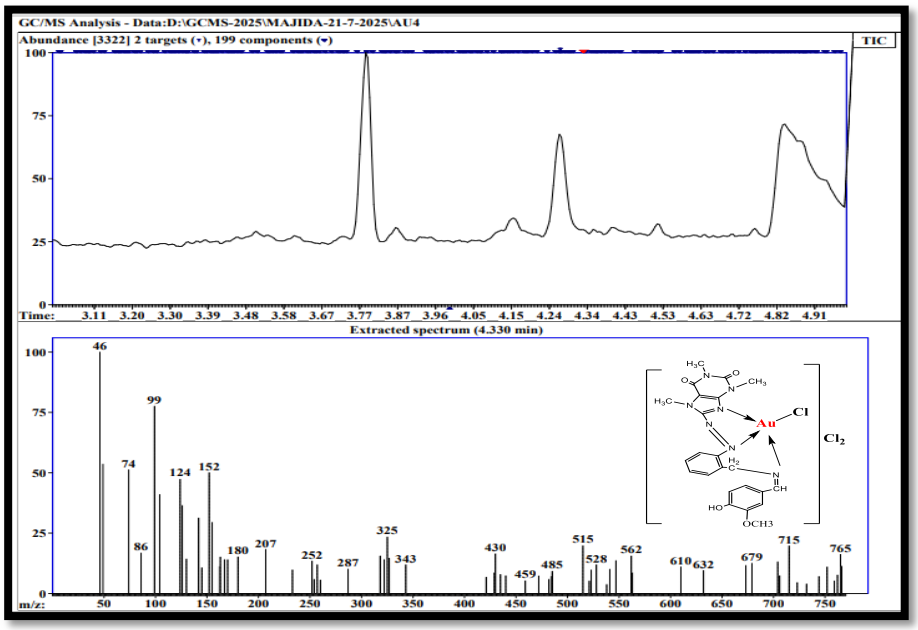

Fig 2. Mass spectrum of [AuLCl]Cl_2 complex

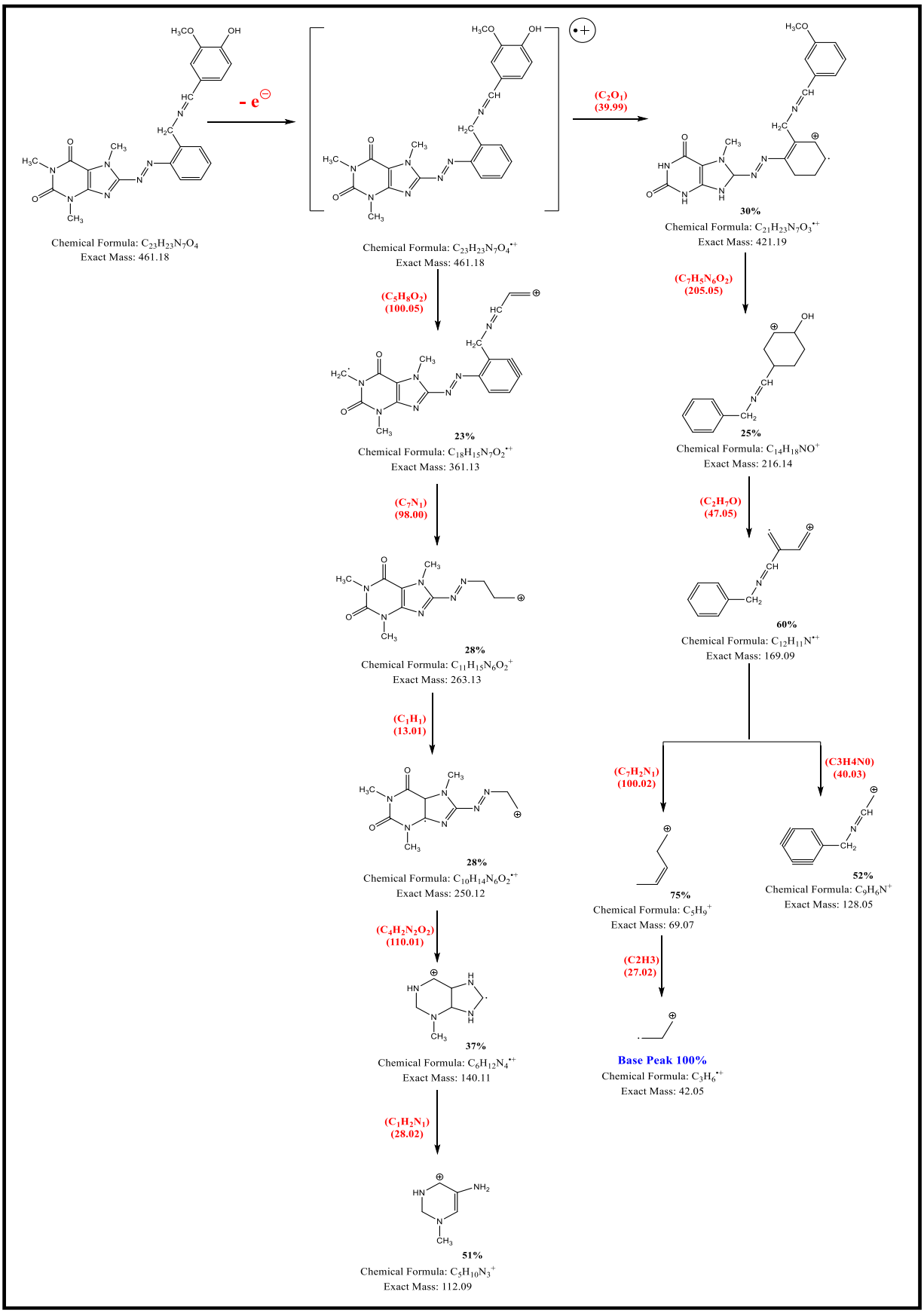

Scheme 3. Mass fractionation pathways of the ligand

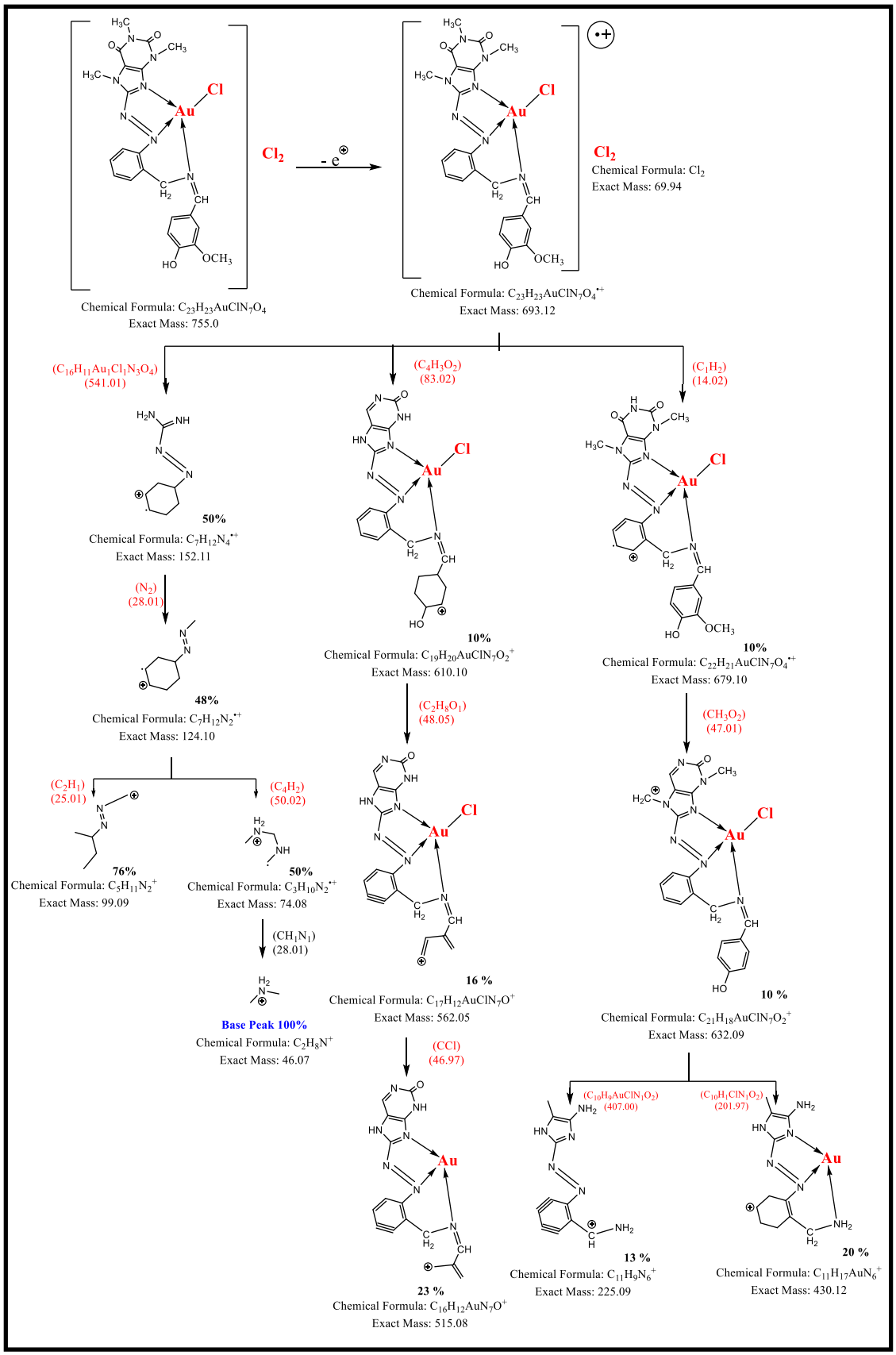

Scheme 4. Mass fractionation pathways of [Au(L)Cl]Cl_2 complex

^{1}H-NMR Spectra

The spectrum of newly synthesized ligand gave a satisfactory data and the molecular structure was assigned on the basic of ^{1}H-NMR chemical shift by using DMSO-d6 as a solvent with TMS as an internal reference. The ^{1}H-NMR spectrum of the ligand showed clear signals involved singlet at δ (2.5) (ppm) belong to the protons of solvent (DMSO-d6) and singlet signal at δ (3.08) ppm which was assigned to H_2O , multiples signals at δ (6.51-7.54) ppm which were assigned to phenyl and heterocyclic protons of rings .Singlet at δ(3.67) ppm belong to the proton of methyl(CH_2), Singlet at δ(3.84) ppm belong to the proton of methyl(N-CH_{3pyrn}). Singlet at δ(4.41) ppm belong to the proton of methyl(N-CH_{3imd}) [20]. Singlet at δ(8.43) ppm belong to the proton of (H–C=N), Singlet at δ(9.79) ppm belong to the proton of (OH)[21] , as shown in Fig.(3).

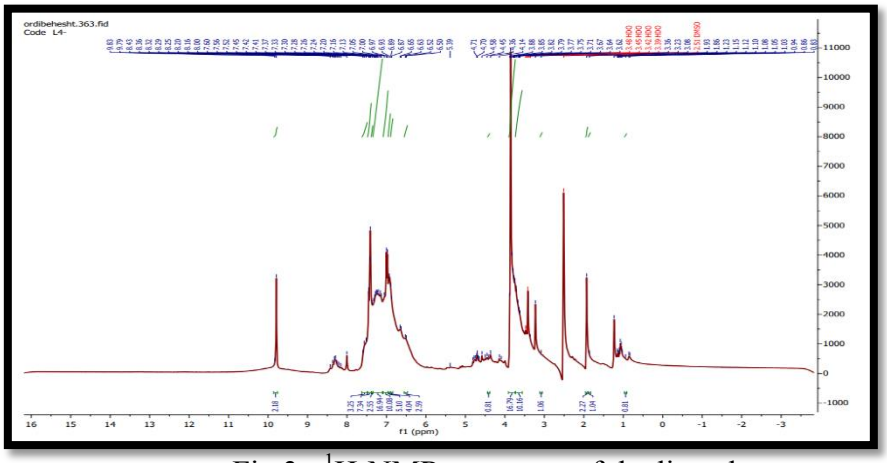

Fig 3 : ^{1}H-NMR spectrum of the ligand

Infrared Spectra studies

The IR spectra of the complexes are compared with that of the free ligand to determine the changes that might have taken place during the Complexation [22,23] all data are listed in table (2).

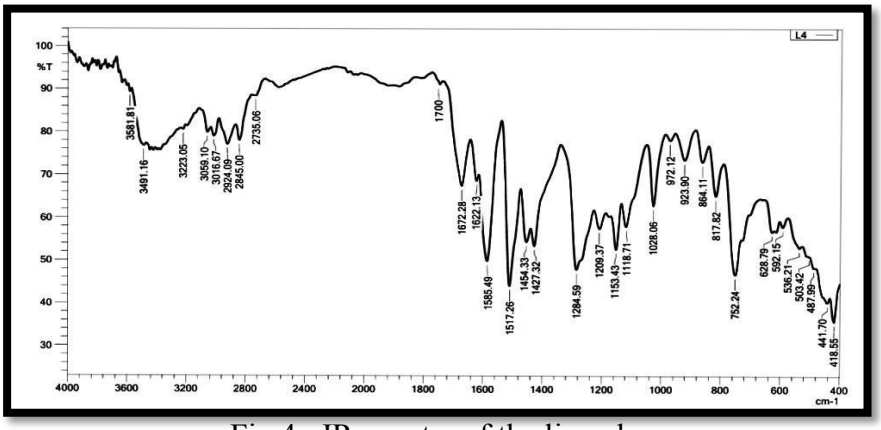

Fig 4 : IR-spectra of the ligand

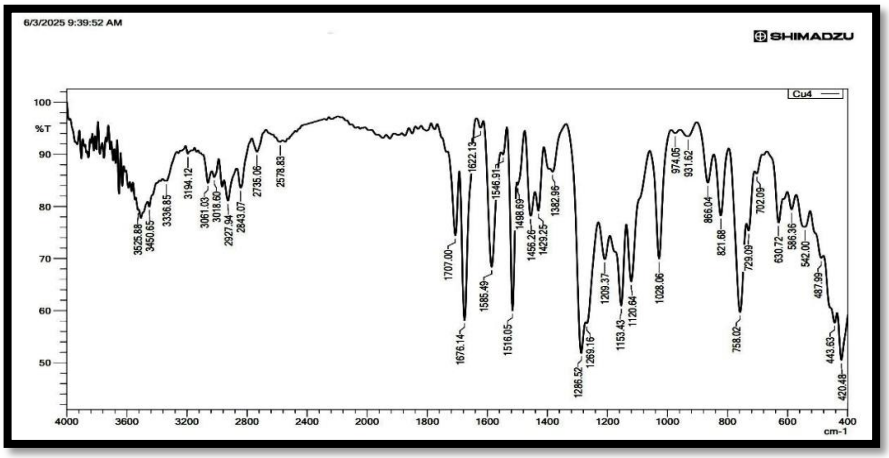

Fig 5 : IR-spectra of Cu (II) complex

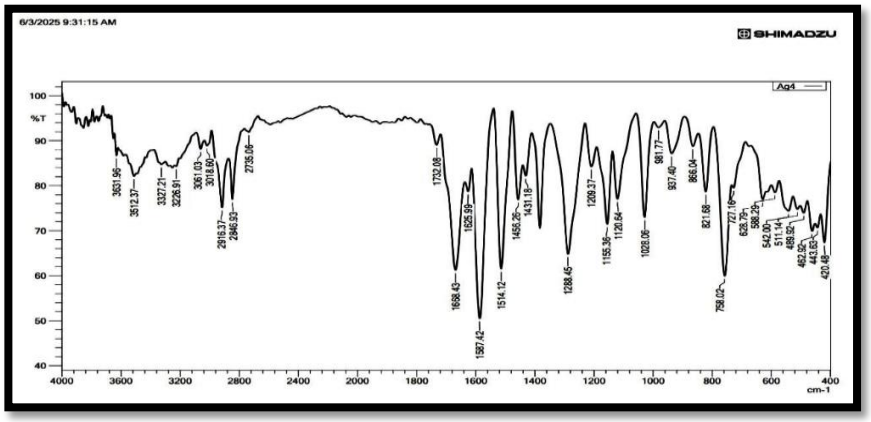

Fig 6 : IR-spectra of Ag(I) complex

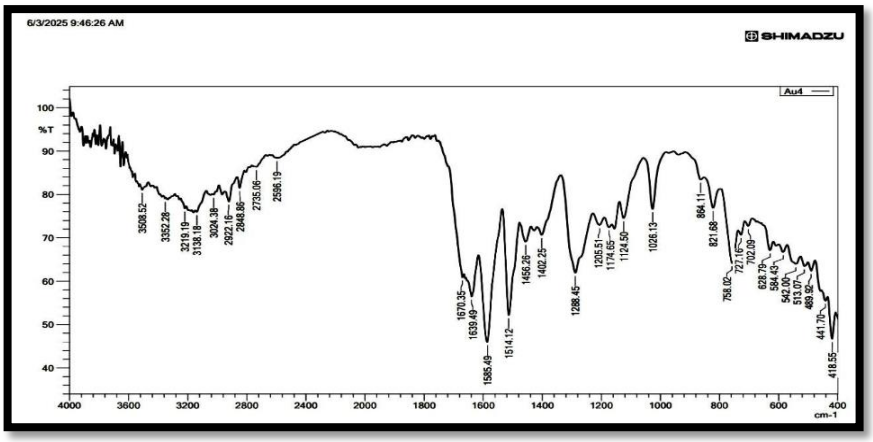

Fig 7 : IR-spectra of Au (□) complex

Table 2 : FTIR spectra frequencies for the new Azo Schiff base ligand and its metal complexes in cm^{-1}

Compound	υ(OH) δ(OH)	υ(C-H) aro	υ(C-H) ali	υ(C=O)	υ(C=N) Schiff	υ(C=N) imid	υ(N=N)	(H_2O) Coord.	(M-N)
$C_{23}H_{23}N_7O_4$	3491 1284	3059 3016	2924	1700	1672	1517	1427	------	------
$[Cu(L)Cl(H_2O)_2]Cl$	3450 1382	3061 3018	2927	1707	1676	1516	1429	931	586-420
$[Ag(L)H_2O]NO_3$	3512 1360	3061 3018	2916	1732	1668	1514	1431	937	588-420
$[Au(L)Cl]Cl_2$	3508 1288	3024	2922	1670	1639	1514	1402	-----	584-418

Elemental Micro Analysis

One of the straightforward and practical analytical techniques for diagnosing chemical compounds is the C.H.N. method, which determines the percentage ratios of carbon, hydrogen, and nitrogen in ligands and their metal complexes formed from them. The flame atomic absorption technique was used to determine the ratios of metallic elements in their complexes [24]. Tables containing the results of these investigations show a strong convergence between the theoretically calculated values and the realistically acquired values. This bolsters the suggested formulations for solid metal complexes on the one hand, and the precision of the added ratios of (metal: ligand) on the other.

From the results obtained, it is clear that the molar electrical conductivity measurements for solutions of Chelate complexes of ions under study with the new ligand and with concentration of (1×10^{-3}) molar per complex at the laboratory temperature and using DMSO as solvent , were ranged from (31.2–73.0)S. cm^2 .mol^{-1} and listed in table (3). All complexes have ionic properties. These results are identical to what was stated in the literature for metallic complexes with ionic properties[25].

Table 3: Molar conductivity and Findings from the exact element and metal ratio study of the ligand (L) complex and its metal complexes

NO	Compounds	MWt	Found / (Calc) (%)				S cm^2 mol^{-1}
			C	H	N	M	
1	(L): $C_{23}H_{23}N_7O_4$	461.48	59.75 (59.80)	4.92 (4.98)	21.20 (21.23)	———	———
2	$[Cu(L)Cl(H_2O)_2]Cl$	632.02	43.61 (43.66)	4.22 (4.27)	15.46 (15.50)	10.01 (10.05)	31.2
3	$[Ag(L)H_2O]NO_3$	649.34	42.46 (42.50)	3.81 (3.85)	17.19 (17.24)	16.57 (16.61)	38.3
4	$[Au(L)Cl]Cl_2$	764.94	36.03 (36.08)	2.95 (3.00)	12.76 (12.81)	25.64 (25.70)	73.0

XRD

XRD gives accurate information on the atomic or molecular makeup of solid-state materials [26]. $[Au(L)Cl]Cl_2$ XRD diffractograms were measured. CuKα radiation was calculated using a wavelength of 1.54060 Å, generator settings of 30 mA/40 kV, and a 2θ range of 0° to 80°. By examining the detected peaks, other diffraction spectrum parameters can be determined using the Xpert High Score software [27]. According to the findings, the chemical had asemicrystalline nature, as shown in Fig. 13. We measured the matching d-spacing values and approximated the significant reflections using Bragg's equation [28]. The formula $n\lambda=2d\sin\theta$ was applied, in where n is an integer (1, 2, 3,...) and d is the distance between the crystalline layers. The wavelength of X-ray CuKα is 1.540598 Å, denoted by the symbol λ. The diffraction angle is represented by the symbol θ. The average diameter of the crystallite and its size distribution were determined using the Debye and Scherrer equation [29]. D kcos =λ β θ (2), where D is the average crystallite diameter, k is the shape factor (0.891), and β is the line broadening at half the maximum intensity (FWHM) [30]. The previously mentioned statistics, such as the density of dissolutions (δ), the microductility (ε), the crystal size (D), and the spacing between the crystalline levels (d), were clearly different from the X-ray spectra. This attests to the coordinating process's existence. In the prepared metal complexe under investigation, we observed that D, ε, and δ had an inverse relationship; the higher D, the lower ε and δ, and consequently, the fewer crystal flaws. Crystalline or semi-crystalline formations are indicated by the strong peaks. The crystal arrangement, crystal lattice characteristics, and crystal planes all affect how intense these peaks are. Furthermore, the reported $[Au(L)Cl]Cl_2$ had experimental average peak radian widths of 43.2306 nm. The compound's crystalline size, with a particle size of less than 100 nm, indicates that it possesses nanostructural qualities [31]. Our earlier measurements of FESEM analysis are supported by the data we received. Table 5 lists the Au(III) complex's crystalline characteristics, and Fig. 8 shows the nano $[Au(L)Cl]Cl_2$ complexes' XRD spectra.

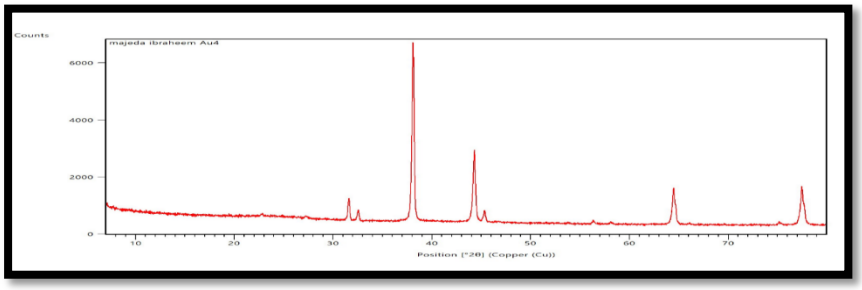

Fig 8 : XRD of $[Au(L)Cl]Cl_2$

Table 4 : The crystalline properties of the Au(III) complex

Compound	Pos. [°2Th.]	Height [cts]	FWHM [°2Th.]	d-spacing [A°]	Rel. Int. [%]	Crystallite Size D (nm)	Dislocation density $\delta*10^{-3}$ $(nm)^2$	Microstrain $\varepsilon * 10^{-3}$	Average size (nm)
$[Au(L)Cl]Cl_2$	23.3568	50.98	2.4261	3.80549	1.14	3.450223	84.005	51.2138	44.50318
	26.0656	39.57	1.5806	3.41583	0.89	5.323322	35.288	29.7952	
	31.5718	546.71	0.1941	2.83153	12.25	43.88761	0.5191	2.99604	
	32.5121	223.63	0.2046	2.75175	5.01	41.73353	0.5741	3.06168	
	38.0625	4463.26	0.2285	2.36227	100	37.94867	0.6943	2.89037	
	44.2543	1889.79	0.2356	2.04506	42.34	37.55958	0.7088	2.52822	
	45.2871	266.14	0.2772	2.00079	5.96	32.04165	0.9740	2.89942	
	56.3211	73.65	0.2116	1.63218	1.65	43.94099	0.5179	1.72470	
	58.1159	38.47	0.2465	1.58598	0.86	38.04335	0.6909	1.9356	
	64.4454	967.91	0.2865	1.44464	21.69	33.82092	0.8742	1.9832	
	66.115	59.53	0.0558	1.41215	1.33	175.2786	0.0325	0.3741	
	75.1652	89.41	0.214	1.26298	2	48.33613	0.4280	1.2132	
	77.435	1095.74	0.2826	1.23153	24.55	37.17673	0.7235	1.5380	

FE-SEM analysis

The surface morphology, particle form, aggregation, and distribution of ligand and mineral complexes are all examined using field emission scanning electron microscopy (FE-SEM) [32]. The cross-sectional distance (500 nm) and magnification force (Mag = 120.000 KX) of the field emission scanning electron microscope (FE-SEM) were employed. Figure: 9 displays FE-SEM pictures of $[Au(L)Cl]Cl_2$ complex. The Au(□)-Complex's FESEM pictures revealed typical spherical heterogeneous crystals with an average size of 58.52 nm. Show that the produced compounds' granules are less than 100 nm in size. By efficiently increasing the surface area, the quantum effect produces new energy levels that facilitate electron mobility [33].

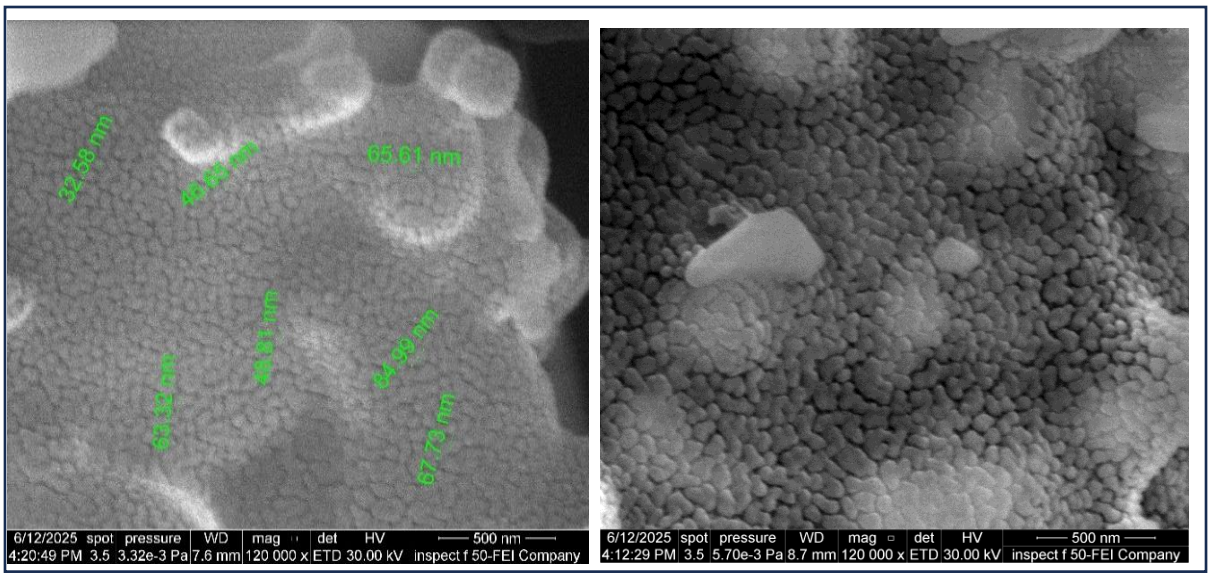

Fig 9 : FESEM images for $[Au(L)Cl]Cl_2$ complexe

Electronic spectra

The UV-Visible spectrum of the new ligand in dimethyl sulfoxide (DMSO) solvent was examined. The absorption spectrum revealed in ligand the first peak at (311 nm, 32154 cm^{-1}), attributed to($\pi \rightarrow \pi^*$) electron transition due to the presence of double bonds in aromatic rings. The second peak appeared at (342 nm, 29239 cm^{-1}), assigned to the ($n \rightarrow \pi^*$) electron transition. resulting from the ligand possessing double bonds with non-bonding electron pairs. The spectrum of the Cu (II) complex in solution showed an absorption peak at (380 nm, 26315 cm^{-1}) was attributed to the charge transfer (ML.CT). This observation aligns with literature findings on the appearance of these bands in octahedral Cu (II) complex spectra. the Ag (I) complex spectrum showed an absorption peak at (364 nm, 27472 cm^{-1}), also related to charge transfer (ML.CT). This observation aligns with the existing research on the occurrence of this band in Ag(I) complex tetrahedral geometry. The Au (III) complex with ligand, this complex exhibited one band at (595 nm, 17699 cm^{-1}) which was assigned to the $^1A_1g \rightarrow {}^1B_1g$ transition and an absorption peak at (439 nm, 22779 cm^{-1}) has been attributed to the ($^1A_1g \rightarrow {}^1Eg$) transition. The Au(III) complex has a diamagnetic moment and square planar geometry.

Table 5: Electronic spectra in (nm) and wave numbers in reciprocal centimeters (cm□¹) For ligand and its complexes

Compouns	λmax (nm)	ύ (cm^{-1})	Transitions	Geometry	Hybridization
(L)$C_{22}H_{20}FN_7O_2$	311 342	32154 29239	π →π* n →π*	----------	----------
[Cu(L)Cl(H_2O)$_2$]Cl	235 272 380	42553 36764 26315	Intra ligand Intra ligand L→M,CT	Distorted Octahedral	Sp^3d^2
[Ag(L)H_2O]NO_3	270 364	37037 27472	Intra ligand M→L,CT	tetrahedral	Sp^3
[Au (L)Cl]Cl_2	231 278 439 565	43290 35971 22779 17699	Intra ligand Intra ligand $^1A_1g \rightarrow {}^1Eg$ $^1A_1g \rightarrow {}^1B_1g$	Square planer	dsp^2

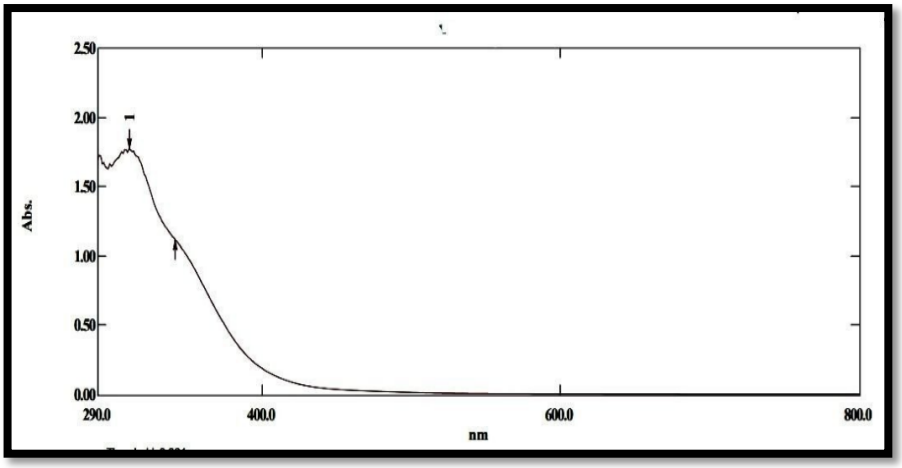

Fig 10 : Ultraviolet-Visible spectrum of the ligand

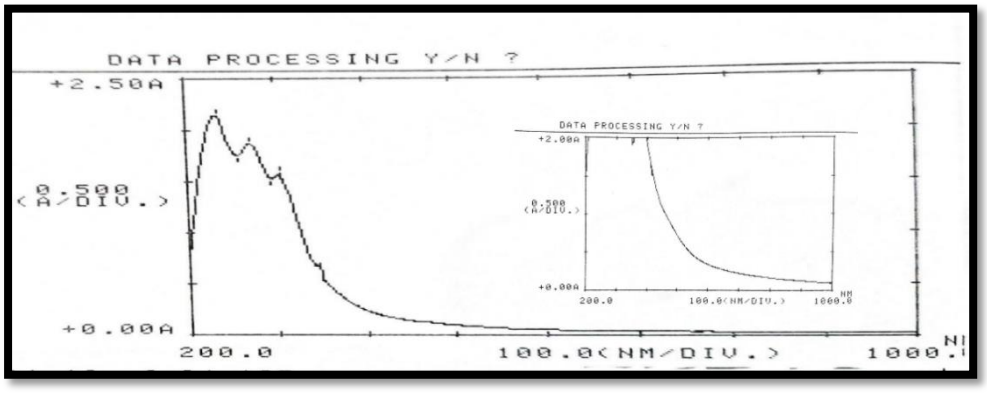

Fig 11 : Ultraviolet-Visible spectrum of Complex [Cu(L)Cl_2 .H_2O]

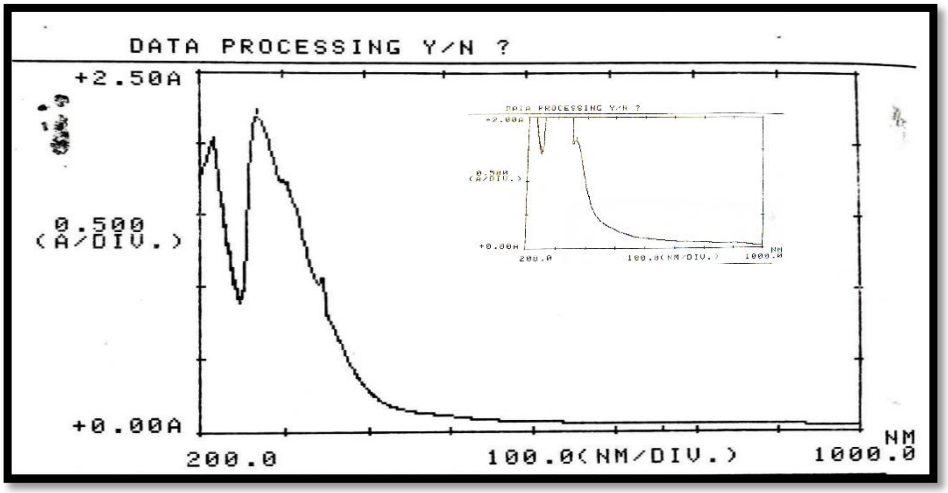

Fig 12 : Ultraviolet-Visible spectrum of Complex $[Ag(L)H_2O]NO_3$

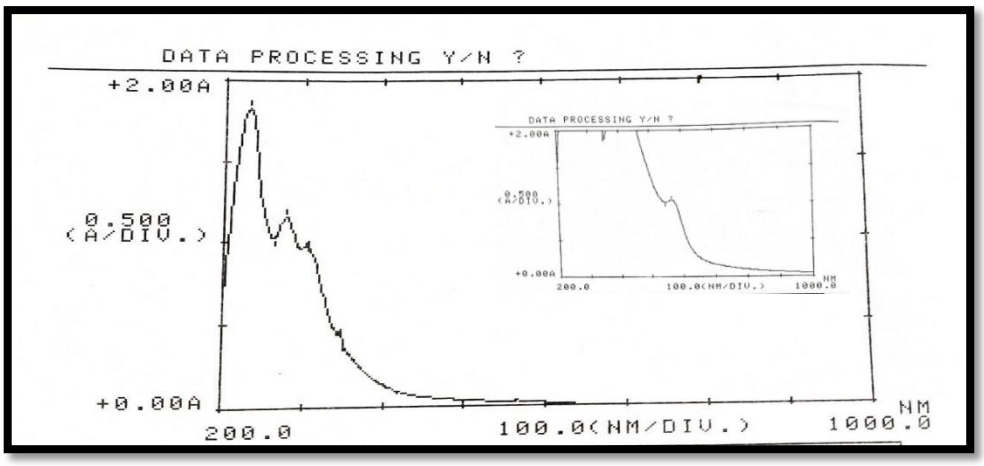

Fig 13 : Ultraviolet-Visible spectrum of Complex $[Au(L)Cl]Cl_2$

The type of metal ion incorporated into the complex, the type and location of substituent groups on the ligand rings, and variations in the available coordination sites that contribute to ligand composition are some of the factors that affect the geometric shapes of metal complexes in their solid form [34]. Square planar, tetrahedral, square-based pyramid, triangular-based pyramid, octahedral, and other geometric shapes have all been suggested. X-ray spectroscopy technique is still essential for verifying the complex's chosen geometric shape.

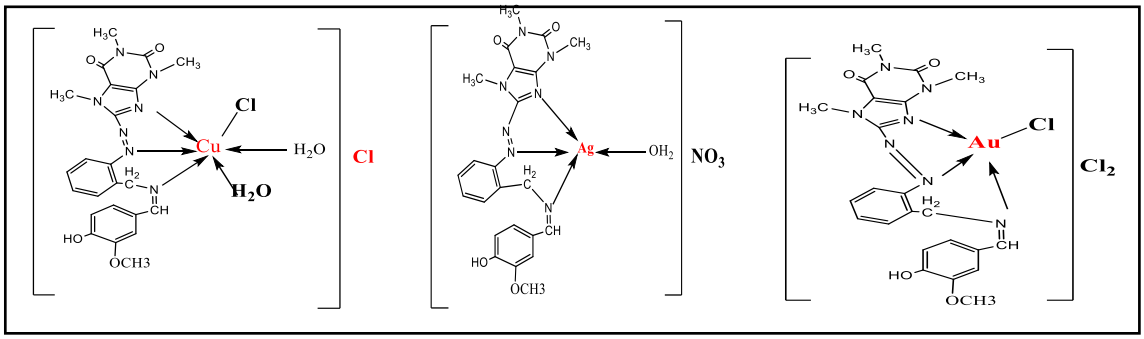

Fig 14 : Stereo form of ligand complexes

Effect of Metal complex on growth of lung cancer cell (A549) and Healthy cells (HDFn)

The impact of the complex $[Au(L)Cl)]Cl_2$ on the growth of lung cancer cell line (A549) and on normal cells (HDFn) was studied[35]. The results showed a lower cell viability percentage (higher inhibition rate) of 72.454% at a concentration of 400 µg/mL for lung cancer cells (A549), while the normal cells (HDFn) exhibited a lower cell viability percentage (higher inhibition rate) of 34.49067% at the same concentration. It was found that increasing the compound concentration decreased cell viability, indicating an increased inhibition rate for both cancerous and normal cell lines[36]. Additionally, the results revealed that the half-inhibitory concentration (IC50) of the $[Au(L)Cl)]Cl_2$ complex for lung cancer cells (A549) was 58.68 µg/mL[37]. This concentration was significantly lower compared to the IC50 for normal cells (HDFn), which was 186.6 µg/mL. These findings suggest that the complex could be used as a treatment for lung cancer (A549), as depicted in Fig. 14

Table 6: The impact of the complex $[Au(L)Cl)]Cl_2$ on the cell lines of lung cancer (A549) and its comparison with normal cells (HDFn) at the same concentration using the MTT test for 24 hours at a temperature of 37°C

Con. (µg.mL^{-1})	Mean Percentage (%) for each cell line			
	Cancerous line cells		Normal line cells	
	A549		HDFn	
	Cell Viability	Cell Inhibition	Cell Viability	Cell Inhibition
25	74.537	25.463	95.17767	4.82233
50	63.92767	36.07233	87.88567	12.11433
100	53.202	46.798	75.54033	24.45967
200	39.622	60.378	72.145	27.855
400	27.546	72.454	65.50933	34.49067
IC50= 58.68			IC50=186.6	

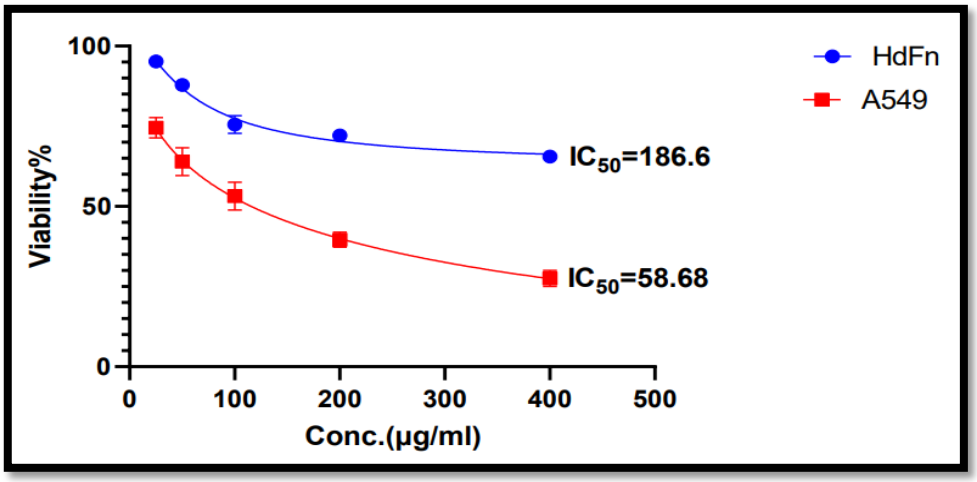

Fig 15 : The half-inhibitory concentration (IC50) of the complexe $[Au(L)Cl]Cl_2$ for A549 and HDFn

References

[1] Kunitake, F., Kim, J.Y., Yagi, S., Yamzaki, Y., Haraguchi, T., and Akitsu, T., 2019, Chiral recognition of azo-Schiff base ligands, their Cu(II) complexes, and their docking to laccase as mediators, Symmetry, 11 (5), 666.

[2] Hadi, M.A., and Kareem, I.K., 2020, Synthesis, characterization and spectral studies of a new azoSchiff base ligand derived from 3,4-diamino benzophenone and its complexes with selected metal ions, Res. J. Adv. Sci., 1 (1), 54–73.

[3] Al-Adilee, K.J., and Hasan, S.R., 2021, Synthesis, characterization and biological activity of heterocyclic azo-Schiff base ligand derived from 2-amino-5-methyl thiazol and some transition metal ions, IOP Conf. Ser.: Earth Environ. Sci., 790 (1), 012031.

[4] Ali, S.A., Elzawi, N.R., and Elyassiry, A.M., 2021, Synergistic and antagonistic effects of azo-Schiff base with some antibiotics on gram-positive bacterial isolates, Res. Rev.: J. Microbiol. Virol., 11 (2), 25–31.

[5] Ashoor, L.S., Majeed, R.A., and Al-Shemary, R.K.R., 2021, Applications of biological of azo-Schiff base ligand and its metal complexes and: A review, Muthanna J. Pure Sci., 8 (1), 74–90.

[6] Jasim, E.Q., Alasadi, E.A., Fayadh, R.H., and Muhamman-Ali, M.A., 2020, Synthesis and antibacterial evaluation of some azo-Schiff base ligands and estimation the cadmium metal by complexation, Syst. Rev. Pharm., 11 (6), 677–687.

[7] J.W. Phillis. The pharmacology of purines in the CNS: Interactions with psychoactive agents, in: Purines, Springer, 1985 45-56.

[8] A.L. Harris, Connell, M. J., Ferguson, E. W., Wallace, A. M., Gordon, R. J., Pagani, E. D., and Silver, P. J. Role of low Km cyclic AMP phosphodiesterase inhibition in tracheal relaxation and bronchodilation in the guinea pig, Journal of pharmacology and experimental therapeutics, 251 (1989) 199-206.

[9] A.a.P. Tenzer, M. Potentiation of DNA-damage-induced cytotoxicity by G2checkpoint abrogators, Current medicinal chemistry-anti-cancer agents, 3 (2003) 35-46.

[10] J.W. Daly. Alkylxanthines as research tools, Journal of the autonomic nervous system, 81 (2000) 44-52.

[11] El-Shehawy, A. A. et al. (2021). "Synthesis, anticancer evaluation, and molecular docking studies of novel azo compounds derived from phenothiazine." Journal of Molecular Structure, 1240, 130634.

[12] Hadi, M.A, Kareem, I.K and Atban,A.M, [2021]: Synthesis And Characterization Of Novel Metal Complexes With New Schiff Base Ligand Derived From 6-Amino Pencillic Acid And Toxicological Studies Of Its Complex With Au(Iii) On Human Cells For Colon Cancer Ls-174, Biochem. Cell. Arch. Vol. 21, Supplement 1, pp. 2477-2488, Doi:

[13] Hadi, M.A, Kareem , I.K. [2020]: synthesis and Characterization of some Transition Matel Complexes with new Azo-Schiff Base Ligand 3,4-bis (((1E,2E)-2-((2-((4-((Z)-(3- Hydroxyphenyl)Diazenyl)Naphthalen-1-yl)amino)ethyl)imino)-1,2Diphenylethylidene)Amino) phenyl)(phenyl)Methanone, Egypt. J .Chem., Vol.63,No.1, pp.301-313.

[14] Hilal, Th.AA., and Kareem, I.K., 2025, Synthesis of Some Metal Complexes with New Heterocyclic Ligand (5-(((2-(3-(1H-indol-3-yl)acryloyl)phenyl)amino)methylene)-2-thiooxodihydropyrimidine-4,6(1H,5H)-dione) and Their Biological Effectiveness as Antioxidant and Anti-Cancer, Indones. J. Chem., 25 (1), 60 – 75.

[15] Arsenijevic.M,Milovanovic.M, Volarevic.V ,Djekovic.A, Kanjevac.T, Arsenijevic.N, Dukic .S and Bugarcic.Z., 2012, Cytotoxicity of gold(III) Complexes on A549 Human Lung Carcinoma Epithelial Cell Line, Medicinal Chemistry, Volume 8, Issue 1, p.2 - 8 .

[16] Al-adilee, K.J., and Hessoon, H.M., 2019, Synthesis, spectral properties and anticancer studies of novel hetrocyclic azo dye ligand derived from 2-amino-5- methyl thiazole with some transition metal complexes, J. Phys.: Conf. Ser., 1234 (1), 012094.

[17] Noor, S.S., and Kareem, I.K., 2024, Exploring the Anticancer Activity of Gold Complex with Newly Ligand (DDIBM): Synthesis, Spectral

Identification and Magnetic Susceptibility of Its Metallic Complexes, Indones. J. Chem., 24 (3), 822 – 834.

[18] Dinnimath, D., Gowda, P. O. O. J. A., & Naik, A. N. W. E. S. H. (2023). Development of organometallic compounds of Schiff bases with diverse applications. International Journal of Pharmacy and Pharmaceutical Sciences, 15(6), 1-15.

[19] Seymore, J. (2022). Molecular characterization of dissolved organic matter in Sao Paulo, Brazil wet deposition by ultra-high resolution mass spectrometry (Doctoral dissertation, Texas A&M University-Corpus Christi).

[20] Hussein,N.A.,and Abbas,A.Kh, 2022, Synthesis, spectroscopic characterization and thermal study of some transition metal complexes derived from caffeine azo ligand with some of their applications, Eurasian Chem. Commun. (4) 67-93.

[21] Obaid,M.I., and Jaafar,W.A, 2022, Formation, Characterization and Thermal Study of Novel Schiff Base Ligand From Sulfonic Acid and Its Complexes with Co(II), Ni(II), Cu(II), Zn(II) and Hg(II) Type NO. Chem. Methodol. 6 (6) 457-462.

[22] Jaafar,W.A, and Saeed.R.S.,2020, Synthesis, Characterization and Corrosion Inhibition

a. Study of New Heterocyclic Compounds and Schiff Base with [Co (II), Ni (II), Cu (II) and Hg (II)] Complexes, Sys Rev Pharm., 11(10):134-143.

[23] Mbarkia,F. and Ammari,F. ,2021, Chemical Modification Of Commercial And Recovered Poly(Vinyl Chloride) With Amino Groups - Adsorption Of Heavy Metals (Cr(III), Pb(II), Cd(II), Or Co(II)) By Modified Pvc Polymers ,J. Mar. Chim. Heterocycl., 20(2), 80-94.

[24] Mahadevi, P., & Sumathi, S. (2023). Schiff base metal complexes: Synthesis, optoelectronic, biological studies, fabrication of zinc oxide nanoparticles and its photocatalytic activity. Results in Chemistry, 6, 101026.

[25] Mohammed,L.A., Hadi, M.A. and Basim,N. A.,2020, Preparation and Characterization of some Complexes with New (Azo-Schiff base) Ligand and Study of Complex as Anticancer Indian Journal of Forensic Medicine & Toxicology, Vol. 14, No. 2.,1298-1305.

[26] Marulanda Cardona, D.M., Wongsa-Ngam, J., Jimenez, H., and Langdon, T.G., 2017, Effects on hardness and microstructure of AISI 1020 low carbon steel processed by high-pressure torsion, J. Mater. Res. Technol., 6 (4), 355–360.

[27] Mustapha, S., Ndamitso, M.M., Abdulkareem, A.S., Tijani, J.O., Shuaib, D.T., Mohammed, A.K., and Sumaila, A., 2019, Comparative study of crystallite size using Williamson-Hall and Debye-Scherrer plots for ZnO nanoparticles, Adv. Nat. Sci.: Nanosci. Nanotechnol., 10 (4), 450.

[28] El-Boraey, H.A., and El-Domiaty, A.M., 2021, Influences of γ-ray irradiation on physico-chemical, structural, X-ray diffraction, thermal and antimicrobial activity of some γ-irradiated N′,N‴- ((Z)-ethane-1,2-diylidine)bis(2- aminobenzohydrazide) metal complexes, Appl. Radiat. Isot., 174, 109774.

[29] Abd Al-Sadda, H.K., Al-Hussainawy, M., and Kyhoiesh H.A.K., 2019, Synthesis, spectral characterization and biological activity of 2-[2¯-(1- amino-1, 5-dinitrophenyl)azo]-imidazole, J. Global Pharma Technol., 11 (7), 165–174.

[30] Serafińczuk, J., Moszak, K., Pawlaczyk, Ł., Olszewski, W., Pucicki, D., Kudrawiec, R., and Hommel, D., 2020, Determination of dislocation density in GaN/sapphire layers using XRD measurements carried out from the edge of the sample, J. Alloys Compd., 825, 153838.

[31] Kyhoiesh, H.A.K., and Al-Adilee, K.J., 2023, Pt(IV) and Au(III) complexes with tridentate-benzothiazole based ligand: Synthesis, characterization, biological applications (antibacterial, antifungal, antioxidant, anticancer and molecular docking) and DFT calculation, Inorg. Chim. Acta, 555, 121598.

[32] Marina M. Safont-Sempere, Gustavo Fernandez, ´ Frank Würthner, Self-sorting phenomena in complex supramolecular systems, Chem. Rev. 111 (9) (2011) 5784–5814.

[33] Y. Li, L. Feng, W. Yan, I. Hussain, L. Su, B. Tan, PVP-templated highly luminescent copper nanoclusters for sensing trinitrophenol and living cell imaging, Nanoscale 11 (3) (2019) 1286–1294.

[34] Wegeberg, C., & Wenger, O. S. (2021). Luminescent first-row transition metal complexes. Jacs Au, 1(11), 1860-1876.

[35] Matveevskaya, V. V., Pavlov, D. I., Samsonenko, D. G., Bonfili, L., Cuccioloni, M., Benassi, E., ... & Potapov, A. S. (2022). Arene-ruthenium (II) complexes with tetracyclic oxime derivatives: synthesis, structure and antiproliferative activity against human breast cancer cells. Inorganica Chimica Acta, 535, 120879.

[36] Al-Ziaydi, A. G., Al-Shammari, A. M., Hamzah, M. I., Kadhim, H. S., & Jabir, M. S. (2020). Hexokinase inhibition using D-Mannoheptulose

enhances oncolytic newcastle disease virus-mediated killing of breast cancer cells. Cancer Cell International, 20, 1-10.

[37] Smith, T., White, T., Chen, Z., & Stewart, L. V. (2024). The KDM5 inhibitor PBIT reduces proliferation of castration-resistant prostate cancer cells via cell cycle arrest and the induction of senescence. Experimental Cell Research, 113991.